

# Electrochemical Synthesis of N-Methylpyrrole and N-Methylcarbazole Copolymer on Carbon Fiber Microelectrodes, and Their Characterization

A. Sezai SARAÇ\*, Erkan DOĞRU, Murat ATEŞ,  
Elif ALTÜRK PARLAK

*Department of Chemistry, Polymer Science and Technology, İstanbul Technical University,  
Maslak, 34469, İstanbul-TURKEY  
e-mail: sarac@itu.edu.tr*

Received 05.10.2005

Copolymer films of N-methylpyrrole (N-MPy) and N-methylcarbazole (N-MCz) were synthesized electrochemically onto single carbon fiber microelectrodes (CFMEs). Deposition conditions on the carbon fiber, influence of the monomer concentrations on the copolymerization of P[N-methylpyrrole-co-N-methylcarbazole] P[N-MPy-co-N-MCz], and the electrochemistry of the resulting homopolymer and copolymers were studied using cyclic voltammetry, FTIR-ATR, in-situ spectroelectrochemistry, a UV-vis spectrophotometer, and a 4-point probe conductometer. The effects of current density, supporting electrolyte type, temperature, and monomer concentrations on the formation of the film were studied. Redox parameters and stability of charged films were obtained by cyclic voltammetry. The most stable copolymer was obtained in lithium perchlorate-acetonitrile electrolytic solution (LiClO<sub>4</sub>/ACN).

**Key Words:** Electrocopolymerization, cyclic voltammogram (CV), carbon fiber microelectrode (CFME).

## Introduction

The electrochemical deposition of conducting polymers on carbon fiber microelectrodes (CFMEs) has been studied with the goal of improving the mechanical properties of these polymers, in order to use them as electrodes in different applications, such as electrochromic displays, batteries, sensors, and capacitors. Interaction and nano-characterization of thin conjugated polymeric films on carbon surfaces, especially on micron-sized carbon fibers, have attracted great interest recently<sup>1,2</sup>, due to the need to modify their surfaces to understand the interfacial properties between the fiber and the matrix.

Polycarbazole, one of many conducting polymers, is known for its good electroactivity, and useful thermal, electrical and photophysical properties<sup>3</sup>. However, a  $\pi$ - $\pi$  electron system along its backbone imparts rigidity to the polymer, and, therefore, makes it infusible and difficult to process. For this reason, it was not initially deployed as widely in devices when compared to other conducting polymers. However,

---

\*Corresponding author

recent advances in synthesis methods have reinvigorated interest in polycarbazole<sup>4</sup>. Investigations related to chemical modification, or in copolymerization of carbazole with other monomers, have led to the use of polycarbazole and its derivatives as redox catalysts, photoactive devices, sensors, electrochromic display, electroluminescent devices, and biosensors<sup>5,6</sup>.

Copolymerization of carbazole and its derivatives with N-methylpyrrole has previously been studied by chemical and electrochemical methods<sup>7</sup>. Due to the combined properties of alkyl substituted pyrrole and carbazole monomers, N-MPy and ethylcarbazole have been copolymerized<sup>8</sup>. Results show that there is an improvement in the electrochemical properties of the copolymer with the incorporation of methylpyrrole. Use of N-methyl substituted pyrrole has the advantage of preventing polymerization through nitrogen, which causes a decrease in conductivity (defect in conjugation of the copolymer is prevented).

In view of the wide spectrum of potential applications, it is clear that a further examination of the electropolymerization conditions, use of different substrates, and the stability of the resulting polymer can help to extend the scope of the technological applications of conducting polymers as thin films. The electrocoating of a range of copolymers with various monomer concentrations has been recently examined using carbon fibers as the microelectrode<sup>9-12</sup>. Electropolymerization of 3-methyl-thiophene with carbazole has been studied, and the surface morphology of the microelectrodes and the relationship between the polymerization parameters have been established<sup>13</sup>.

Since electronic properties are considered, copolymerization starts from two monomers that contain an alkyl group. This arrangement seems more favorable. The presence of an alkyl group gives solubility to copolymers obtained electrochemically<sup>14</sup>. Polymers containing N-alkyl-3-6-carbazole units were found to be soluble in organic solvents<sup>15</sup> and could be then easily processed. Electrochemical synthesis has become the preferred method for preparing electrically conducting polymers because of its simplicity and reproducibility. The advantage of electrochemical polymerization is that the reactions can be carried out at room temperature<sup>16</sup>.

Factors affecting the electrocopolymerization are investigated to control experimental conditions. Electrocopolymerization is controlled by a variety of parameters, i.e. concentration, monomer feed ratio, temperature, electrolyte type, number of carbon fibers, and scan rate. Carbon fibers as micron-sized electrodes, the nature of copolymeric films, and their structure and compositions play an important role in understanding the effect of the electrochemical conditions used for coating the fiber on the final properties of the modified carbon surface<sup>17</sup>. With this aim in mind, we recently studied the electrografting of copolymers with conductive and non-conductive portions onto carbon fibers<sup>18-21</sup>.

In this work, the polymerization of N-methylpyrrole with N-methylcarbazole was achieved electrochemically. The electrocopolymerization of methylcarbazole with methylpyrrole was studied to improve the electrochemical properties of N-MCz. The polymers (P[N-MPy], P[N-MCz] and P[N-MPy-co-N-MCz]) obtained in different solutions were analyzed using cyclic voltammetry (CV).

## Experimental

### Materials

N-methylpyrrole (N-MPy, >98%), sodium perchlorate (NaClO<sub>4</sub>, > 98%), lithium perchlorate (LiClO<sub>4</sub>, > 98%), propylene carbonate (PC, >99%), and acetone (99.7%, Purex PA) were obtained from Merck. Acetonitrile (ACN) was from Carlo Erba. Potassium perchlorate (KClO<sub>4</sub>), tetrabutylammonium perchlorate

(TBAP) and tetraethyl ammonium perchlorate were obtained from Aldrich. High Strength (HS) carbon fibers C320000A (CA) (Sigri Carbon, Meitingen, Germany) containing 320,000 single filaments were used as the working electrodes. Indium tin oxide (ITO) coated glass slides (0.7 cm x 5 cm,  $R \leq 10 \text{ ohm cm}^{-2}$ ) were from Delta Technologies (USA), and were used for some of the in-situ spectroelectrochemical studies. All chemicals were high-grade reagents and were used as received.

## Cyclic Voltammetry

Cyclic voltammograms of the polymers were obtained with a Parstat 2263 potentiostat, which is a self-contained unit that combines potentiostatic circuitry with phase-sensitive detection (Faraday cage with BAS Cell Stand C<sub>3</sub>), in a 3-electrode system setup employing CFME as the working electrode, platinum wire as the counter electrode, and a silver wire pseudo-reference in LiClO<sub>4</sub> / PC or NaClO<sub>4</sub> / ACN (0.1 M). The pseudo-reference was calibrated externally using a 5 mM solution of ferrocene (Fc / Fc<sup>+</sup>) in the electrolyte [ $E_{1/2}(\text{Fc} / \text{Fc}^+) = +0.13 \text{ V}$  vs. silver wire in 0.1 M LiClO<sub>4</sub>/ PC]. Polymerization reactions were also performed galvanostatically (0.2 A) in PC or ACN solution containing 0.1 M LiClO<sub>4</sub> or NaClO<sub>4</sub> and monomers.

## Preparation of the CFME

A single filament of the CFME was used as a working electrode. All the electrodes were prepared by using a 3 cm length of the CFME (diameter  $\sim 7 \mu\text{m}$ ) attached to a copper wire with Teflon tape. Only 1.0 cm of the carbon fiber was dipped into the solution to keep the electrode area constant ( $\sim 0.0022 \text{ cm}^2$ ). The rest of the fiber was covered with the Teflon tape.

## The Solid State Conductivity Measurements

Electrochemical syntheses of films were performed galvanostatically on a Pt plate electrode with a surface area of  $1.68 \text{ cm}^2$ . Solid state electrical conductivity measurements were carried out for films removed from the electrode surface. A Keithley 617 electrometer was connected to a 4-point probe head with gold tips. Electrical conductivity was calculated from the following equation:

$$\sigma = V^{-1} / (\ln 2 / \pi \cdot d_n), \text{ where } d_n \text{ is thickness in cm, } V \text{ is applied potential in V, and } I \text{ is current in A.}$$

## FTIR-ATR and UV-vis Spectrophotometry

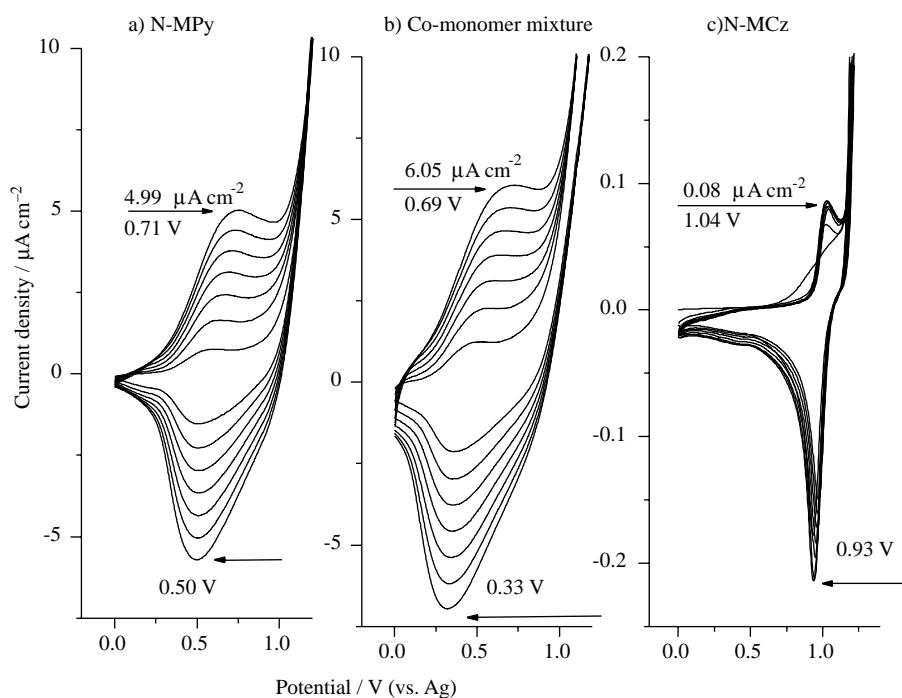
Electrografted CFMEs (with a single grafted CF) were analyzed by FT-IR reflectance spectrometry (Perkin Elmer, Spectrum One B, with an ATR attachment Universal ATR-with ZnSe crystal).

UV-Visible spectra were obtained both for electrochemically coated ITO glass and oligomers were formed in solution by using a Shimadzu 160 A recording spectrophotometer.

## Results and Discussion

### Electropolymerization of N-MPy, N-MCz, and the monomer mixture by CV on CFMEs

The cyclic voltammograms of N-MPy, N-MCz, and the monomer mixture of thin films electrochemically deposited on CFME (at  $100 \text{ mV s}^{-1}$  scan rate) recorded in  $0.1 \text{ M NaClO}_4 / \text{PC}$  are shown in Figures 1a-1c, respectively. Current densities vs. potential changes were electrochemically obtained using alkyl-substituted monomers, N-MPy and N-MCz (structures are given in Table 1). They intensified during repetitive scans, indicating the doping-dedoping of the electroactive film. The oxidation potential of the co-monomer mixture is obtained at  $0.69 \text{ V}$ , which is smaller than the oxidation potentials of N-MCz ( $1.04 \text{ V}$ ) and N-MPy ( $0.71 \text{ V}$ ) when using an electrogrowth mechanism. The onset potentials of N-methylpyrrole, N-methylcarbazole, and a mixture of both monomers were obtained at  $0.84$ ,  $1.00$  and  $0.87 \text{ V}$  on CFMEs by linear sweep voltammogram, respectively (Figure 2). CV of the monomer mixture shows different redox behavior, and oxidation potentials than monomers.

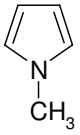
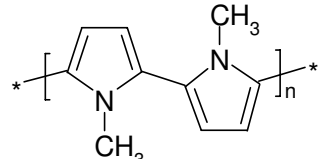
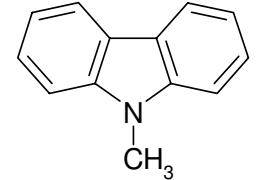
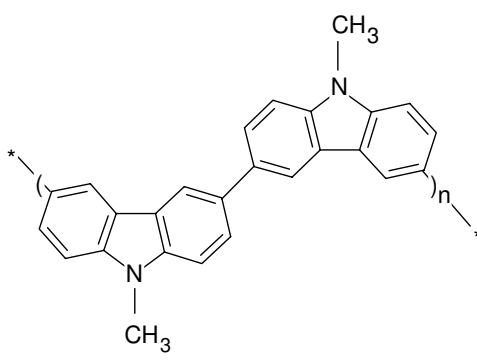
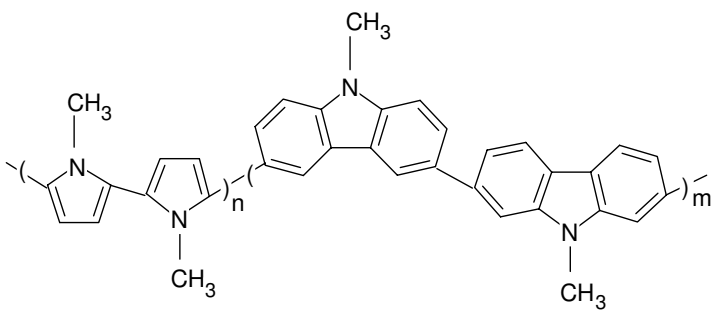


**Figure 1.** CV for the oxidation of a) N-MPy, b) co-monomer mixture, c) N-MCz on CFME in  $0.1 \text{ M NaClO}_4 / \text{PC}$  at  $100 \text{ mV s}^{-1}$ . Using multiple cycles (7), Potential range:  $0\text{-}1.2 \text{ V}$ ,  $[\text{MPy}]_0 = 10^{-3} \text{ M}$ ,  $[\text{N-MCz}]_0 = 10^{-3} \text{ M}$ ,  $[\text{Co-monomer mixture}]_0 = 10^{-3} \text{ M}$ .

### Effect of scan rate on modified CFME in monomer free electrolyte Scan rate dependence

The current density is linearly proportional to voltage, and the scan rate indicating all electroactive sites are electrode supported. The cyclic voltammogram of  $\text{P}[\text{N-MPy-co-N-MCz}]$  coated CFME in monomer-free electrolyte shows one oxidation potential at  $0.7 \text{ V}$  having linear dependence with the scan rate. In monomer

**Table 1.** Structure and abbreviation of monomers and their polymers.

Structure	Monomers	Polymers
	N-MPy	
		P[N-MPy]
	N-MCz	
		P[N-MCz]
	N-MCz, N-MPy	P[N-methylpyrrole- co-N- methylcarbazole]

free solution, the CV of P[N-MPy], P[N-MCz] (Figures 3a and b) and P[N-MPy-co-N-MCz] (Figure 4) are recorded at  $100 \text{ mV s}^{-1}$ . During the first few cycles for the copolymer, oligomeric species or small polymer

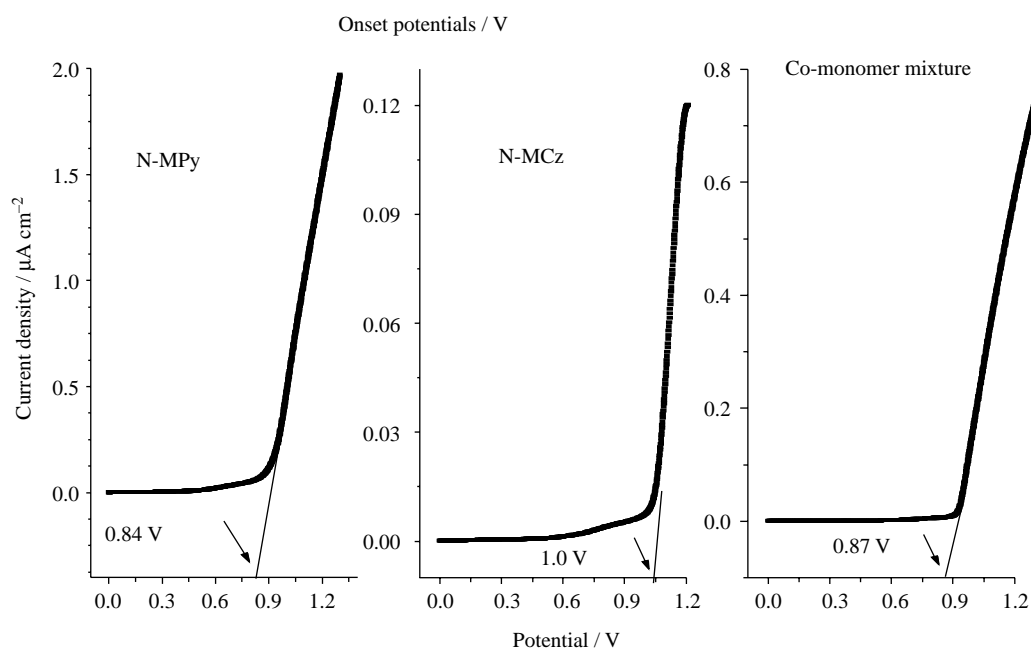


**Figure 2.** Onset potentials of a) N-MPy, b) N-MCz, c) co-monomer mixture by linear sweep voltammogram on CFME in 0.1 M NaClO<sub>4</sub> / PC at 100 mV s<sup>-1</sup>. Potential range: 0-1.2 V, [N-MPy]<sub>0</sub> = 10<sup>-3</sup> M, [N-MCz]<sub>0</sub> = 10<sup>-3</sup> M, [Co-monomer mixture]<sub>0</sub> = 10<sup>-3</sup> M.

chains formed and dissolved during the oxidation and reduction cycle, leaving longer polymer chains, which remain adhered on the CFME surface. Therefore, the charge stabilized after a few cycles. The dissolution of smaller species was not observed for polymers formed at slower rates, indicating that the longer chains were obtained at slow rates allowing a longer structure of polymer chains. This is related to the time of polarization of the electrode. The peak current ( $i_p$ ) for a reversible voltammogram at 25 °C is given by the following equation:

$i_p = (2.69 \times 10^5) \cdot A \cdot D^{1/2} \cdot C_0 \cdot v^{1/2}$ , where  $v$  is the scan rate,  $A$  is electrode area,  $D$  is the diffusion coefficient of electroactive species, and  $C_0$  is the concentration of electroactive species in the solution. Peak current is proportional to  $v^{1/2}$  in the range of scan rates where diffusion control applies<sup>22</sup>. The scan rate dependence of the anodic and cathodic peak currents shows a linear dependence on scan rate for copolymer against  $v^{1/2}$  (Figure 5). This demonstrates that both the electrochemical process is diffusion controlled and has thin film formation (dependence on  $v$  might also be an indication for thin film formation (inset Figure 5)). This shows that the electrochemical process is extremely reversible even at high scan rates. There is a deviation from linearity beyond 100 mV s<sup>-1</sup>. This demonstrates that the electrochemical process is not diffusion limited and is extremely reversible even at high scan rates<sup>23</sup>. The ability to be switched reversibly in a non-diffusion limited process at scan rates as high as 200 mV s<sup>-1</sup> is unusual for conducting polymers and may stem from the thickness of the polymer films.

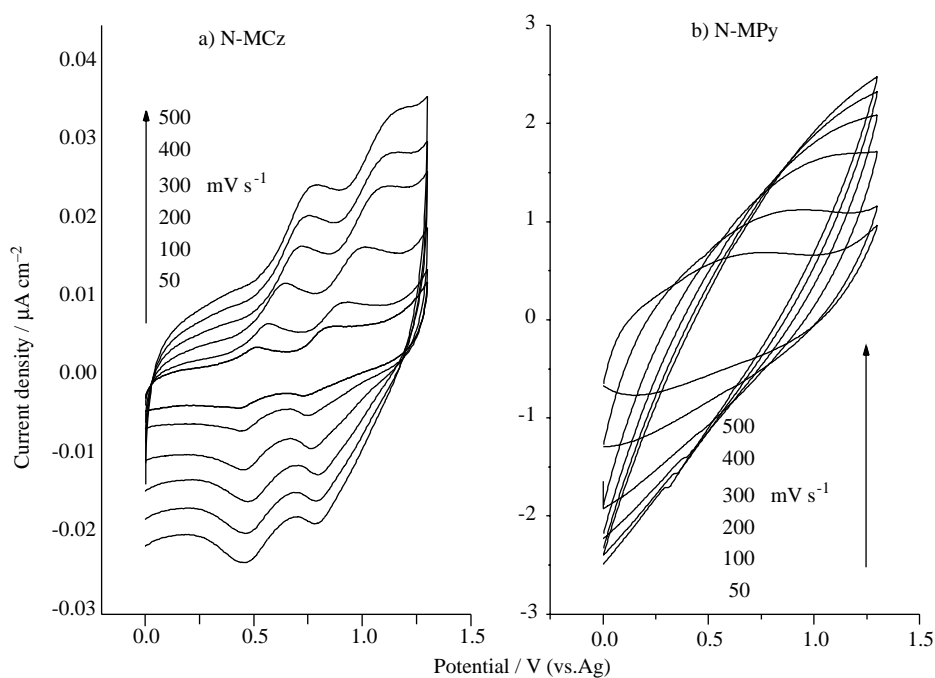


**Figure 3.** Scan rate dependence of cyclic voltammogram of a) P[N-MCz] and b) [N-MPy] electrochemically polymerized on CFME in 0.1 M  $\text{NaClO}_4$  / PC solution using multiple cycles (8) and only the fourth cycle is shown in monomer-free solution by cyclic voltammetry. Scan rates: 50, 100, 200, 300, and 500  $\text{mV s}^{-1}$ .

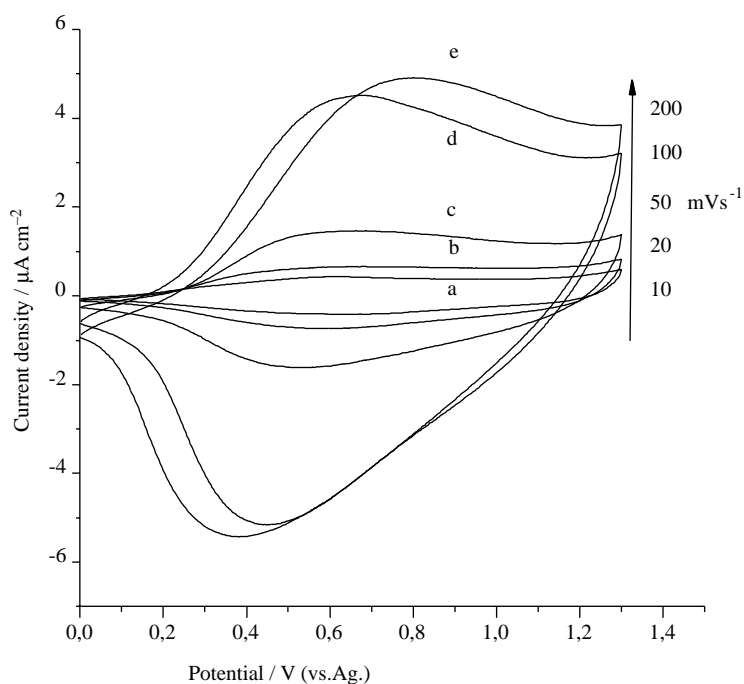


**Figure 4.** Scan rate dependence of cyclic voltammogram of P[N-MPy-co-N-MCz] formed by 8 cycles at a) 10  $\text{mV s}^{-1}$ , b) 20  $\text{mV s}^{-1}$ , c) 50  $\text{mV s}^{-1}$ , d) 100  $\text{mV s}^{-1}$ , e) 200  $\text{mV s}^{-1}$  in a 0.1 M  $\text{NaClO}_4$  / PC solution. All samples were subsequently cycled 8 times and only the fourth cycle is shown in monomer-free solution.

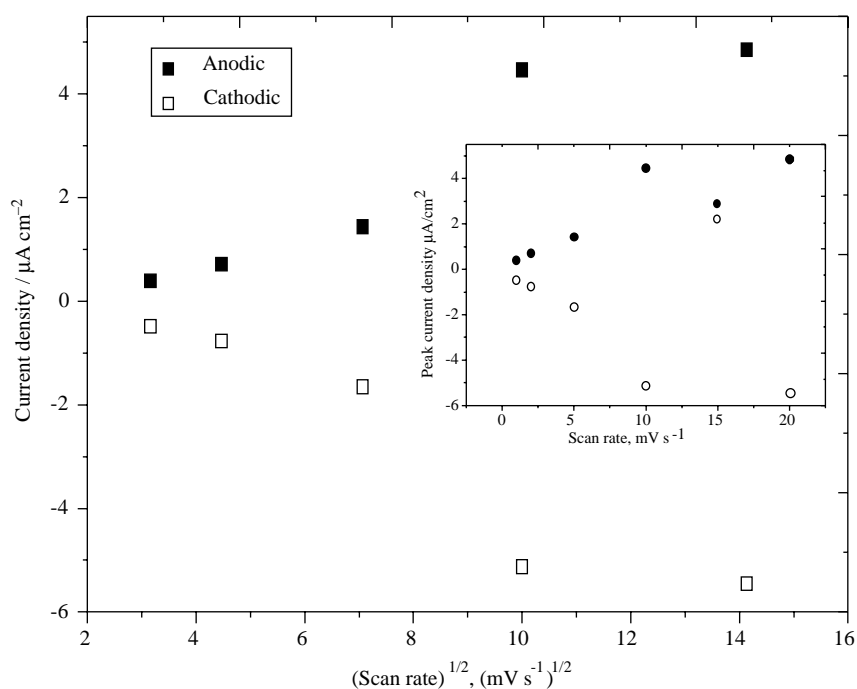


**Figure 5.** Plots of anodic and cathodic peak current density vs. the square root of scan rate. Inset: Plots of anodic and cathodic peak current density vs. scan rate dependence of the copolymer film in monomer free solution in 0.1 M NaClO<sub>4</sub>/ PC.

### Effects of feed ratios on copolymer during electrogrowth

The cyclic voltammogram of P[N-MPy] with different initial monomer concentrations indicates that concentration plays a very important role in the polymerization reaction. The initial feed ratio of [N-MCz]<sub>0</sub>/[N-MPy]<sub>0</sub> for the copolymer formation increases from 0.01 to 10, while the anodic peak potential rises from 0.37 to 0.43 V. Anodic and cathodic current density ratio also increases from 1.04 to 1.08 by initial feed ratio increase. In these experiments, initial N-MPy concentration was held constant, at 10<sup>-2</sup> M, but N-MCz concentration changed from 10<sup>-4</sup> to 10<sup>-1</sup> M (Table 2).

**Table 2.** E<sub>p<sub>a</sub></sub>/ E<sub>p<sub>c</sub></sub>, anodic and cathodic peak potentials (E<sub>p<sub>a</sub></sub>, E<sub>p<sub>c</sub></sub>) in monomer free electrolyte obtained from CV of homopolymer and copolymers. N-MCz concentration changed from 10<sup>-4</sup> to 10<sup>-1</sup> M. [N-MPy]<sub>0</sub> = 10<sup>-2</sup> M.

Polymer	[N-MCz] <sub>0</sub> /[N-MPy] <sub>0</sub> <sup>a</sup>	E <sub>p<sub>a</sub></sub> , V	E <sub>p<sub>c</sub></sub> , V	ΔE, V	I <sub>p<sub>a</sub></sub> / I <sub>p<sub>c</sub></sub>
P[N-MPy]	-	0.45	0.34	0.11	-
P[N-MCz]	-	0.35	0.15	0.10	-
P[N-MPy-co-N-MCz]	0.01	0.37	0.35	-	1.04
P[N-MPy-co-N-MCz]	1	0.40	0.34	0.06	1.02
P[N-MPy-co-N-MCz]	10	0.43	0.33	0.10	1.08

<sup>a</sup>Initial feed ratio of N-MCz / N-MPy

Increases in current densities obtained from electrogrowth of copolymers on the electrode surface (current density vs. scan numbers) are greater than that of P[N-MCz] (Figure 6). As N-MCz initial monomer concentrations in the copolymer increase, current densities approach the homopolymer of N-MCz.



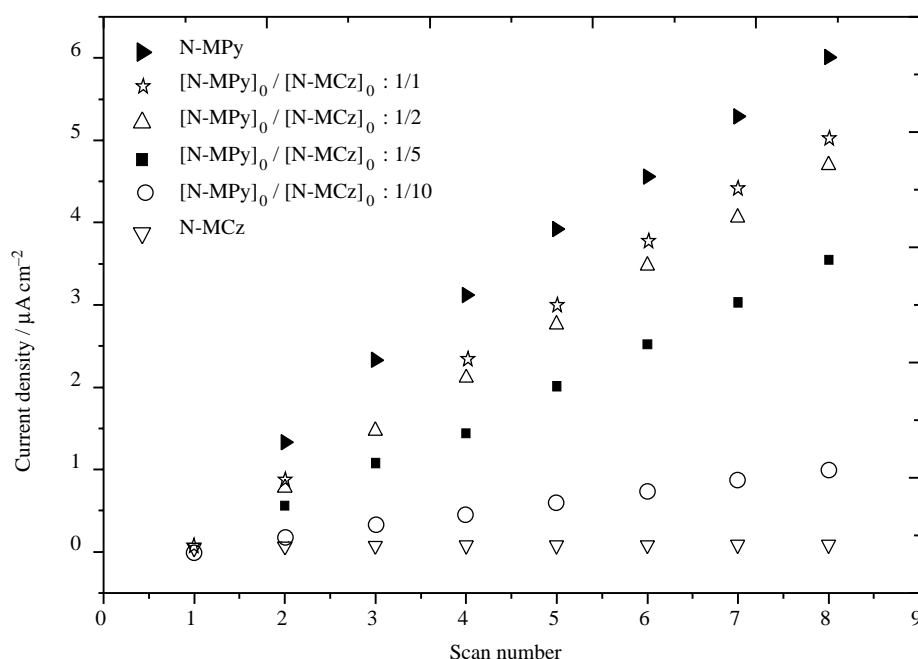


**Figure 6.** Electrochemical coating of N-MPy, N-MCz and N-MCz-co-N-MPy mixture at different initial feed ratios: Current density vs. scan number.

### Determination of number of carbon fibers

To study with a known number of single CFMEs, counting the number of CFME (diameter  $\sim 7 \mu\text{m}$ ) is very difficult. The initial work was carried out by counting the fibers using a microscope. CV experiments were performed on counted carbon fibers and the current vs. carbon fiber numbers are plotted to determine the current of each fiber during the electrogrowth of polymer. However, the limitation of this method is that one has to always dip fibers to the same depth in the electrolyte solution. The currents are taken from switching potentials and for the determination of unknown CFME samples. One would be able to determine the number of these fibers by simply dividing the current of several fibers by the current of a single fiber (Figure 7).

### Effects of monomer concentration on the yield and conductivity (Galvanostatically)

Both the solid state conductivity and yield vs. initial monomer concentration for the homopolymer of P[N-MCz] are given in Figure 8. The results indicate that an increase in N-MCz concentration from  $10^{-3}$  to  $10^{-2}$  M leads to an increase in the solid state conductivity. This increases the thickness of the thin polymer film. Solid state conductivity increases from  $1.21 \pm 0.05 \text{ mS cm}^{-1}$  to  $3.50 \pm 0.05 \text{ mS cm}^{-1}$ . Percent yield was also increased from 9.7% to 59.1% by increasing initial monomer concentration. It could be observed that the changes in the concentration caused a simultaneous increase in conductivity. In the case of the copolymer, conductivity decreased with the increase in N-MCz concentration (yields, feed ratios) (Figure 9). When N-MCz concentration increases 10-fold, conductivity decreases from  $4.20$  to  $0.43 \text{ mS cm}^{-1}$ . An increase in N-MCz initial concentration results in an increase in yield but a decrease in conductivity. The

yield increase indicates that N-MCz is incorporated into the copolymer structure while the conductivity of the copolymer decreases.

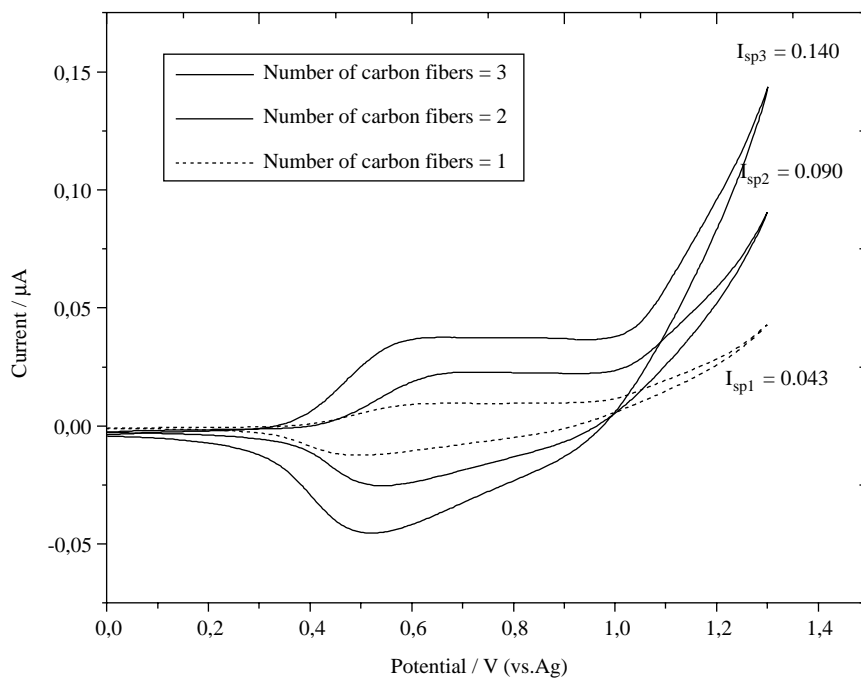


**Figure 7.** Electrochemical coating of P[N-MPy-co-N-MCz] by CV with different numbers of carbon fibers in 0.1 M NaClO<sub>4</sub> / ACN solution using multiple cycles and eighth cycle (Scan rate: 100 mV s<sup>-1</sup>, Potential range: 0-1.3 V).

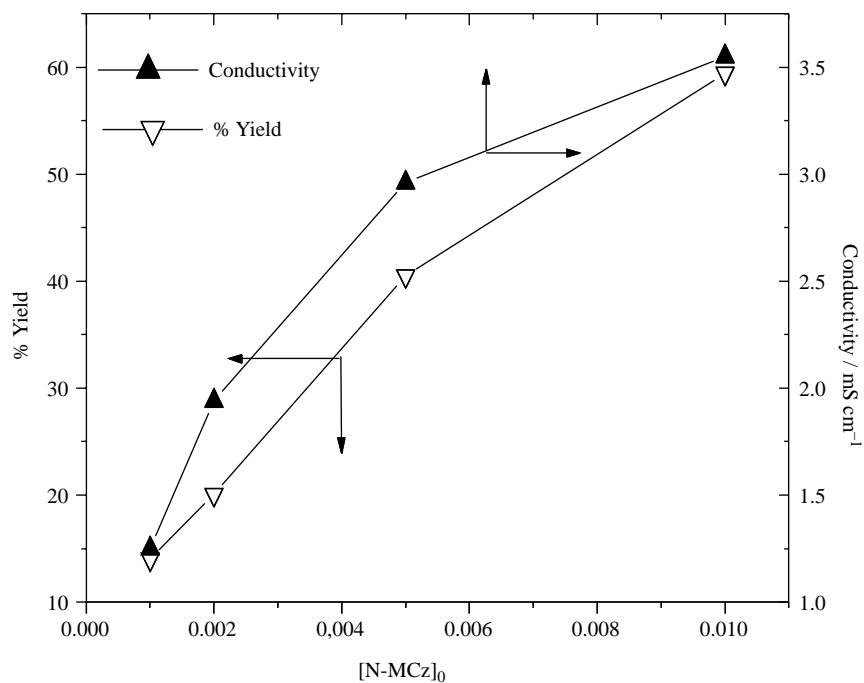


**Figure 8.** Effect of initial monomer concentration [N-MCz]<sub>0</sub> on P[N-MCz], conductivity and % yield.

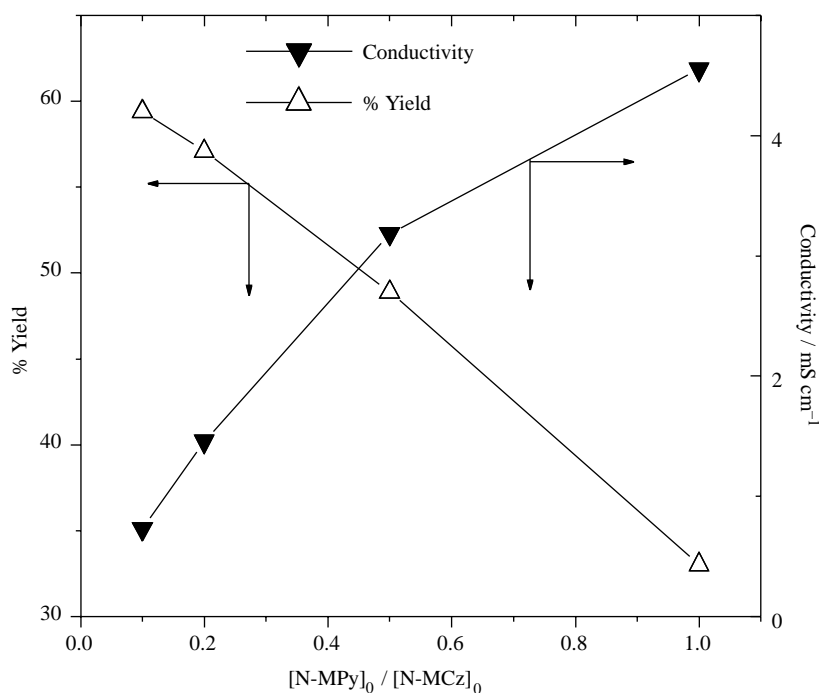


**Figure 9.** Effect of feed ratio of  $[N-MCz]_0/[N-MPy]_0$  on solid state conductivity and yield.  $[N-MPy]_0 = 0.01$  M.

## Effects of temperature, and cation on modified CFME

### Effect of the temperature

By decreasing the temperature from 20 to 0 °C, the anodic peak potential of the copolymer decreased from 0.53 to 0.46 V. At 20 °C, the polymer shows better reversibility ( $I_{p_a}/I_{p_c} = 0.88$ ) than the others (0, 5, and 10 °C). Among the conditions of the copolymer that were studied potentiodynamically at different temperatures, the highest current densities were obtained at 20 °C (Figure 10).

### Effect of the cation

The electrochemical properties were analyzed in the presence of different cations ( $Na^+$ ,  $Li^+$ ,  $K^+$ , TBAP, and TEAP). Ionization potentials ( $I_p$ ) of homopolymer and copolymer electrodes were calculated as suggested in the literature.<sup>24,25</sup>

$I_p = (E_{ox} + 4.4)$  eV, ionization potential of P[N-MPy-co-N-MCz] is between the homopolymers, and the peak potentials are shown in Table 3. It indicates that the removal of an electron is easier than in P[N-MCz], and so decreased the oxidation potential of monomer. Furthermore, the conductivity measurements indicated that copolymer conductivity is higher than that of P[N-MCz]. It is shown that the copolymer has a structure different than that of the two homopolymers. For all cations, a linear dependence was found between the decreases in the anodic peak current density measured at a fixed concentration of cation (Table 4). These effects were attributed to a shielding of the conjugated backbone caused by the potential barrier formed by the host guest complex. The size of the cation can have an influence on the polymer conductivity. It is shown that the larger the cation, the lower the conductivity of the polymer. The current density of anodic peaks for each electrolyte is directly proportional to the applied total charge. Moreover, there might

be a similar relation between the ionization potential of cations and anodic current density (CV results). However,  $\text{Na}^+$  cation shows a distinctive property contrary to the relation (Table 4).

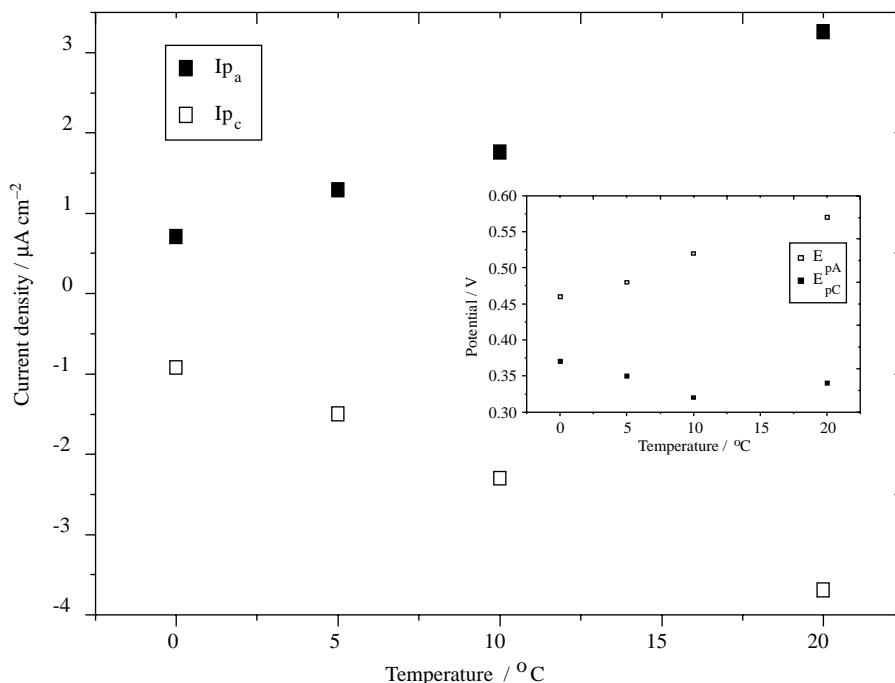


**Figure 10.** Anodic and cathodic current densities vs. temperature of copolymer coated electrochemically on CFME. Inset: Graph of anodic and cathodic peak potentials vs. temperature.

**Table 3.**  $E_{pa}$ ,  $E_{pc}$ ,  $\Delta E$ ,  $E_{ox}$ ,  $I_p$  values of polymers in the range of 0 to 1.3 V.

Polymer	$E_{pa}$ , V	$E_{pc}$ , V	$\Delta E$ , V	$E_{ox}$ , V	$I_p$ , eV
P[N-MPy]	0.75	0.50	0.25	0.10	4.50
P[N-MCz]	1.02	0.94	0.08	0.90	5.30
P[N-MPy-co-N-MCz]	0.74	0.33	0.41	0.26	4.66

**Table 4.** Relation of some electrolytes with total charge-anodic peak current density (coating and in monomer free) - Ionization energy.

Electrolytes / ACN	$\Delta Q$ (mC) <sup>a</sup>	$I_{pa}(\mu\text{Acm}^{-2})^b$	$I_{pa}(\mu\text{Acm}^{-2})^c$	$E_i$ (eV) <sup>d</sup>
$\text{NaClO}_4$	12.77	8.46	1.92	5.14
$\text{LiClO}_4$	8.77	3.43	3.33	5.39
$\text{KClO}_4$	5.36	2.79	1.67	4.34
TBAP	3.96	2.12	-	-
TEAP	3.46	1.66	-	-

<sup>a</sup> Total charge obtained in polymer growth.

<sup>b</sup> Anodic peak current density obtained in polymer growth.

<sup>c</sup> Anodic peak current density obtained in monomer free electrolyte at 50<sup>th</sup> cycle.

<sup>d</sup> Ionization energy of cations.

### FTIR-ATR measurements

The FTIR-ATR spectra of P[N-MPy], P[N-MCz], and P[N-MPy-co-N-MCz] were obtained from the surface of the electrocoated CFMEs by reflectance measurements (only a few modified CFMEs). Absorption bands of each spectrum are given in Figure 11. Characteristic peaks were observed at 1517-1415  $\text{cm}^{-1}$ , 1385-1297  $\text{cm}^{-1}$ , and 771  $\text{cm}^{-1}$ , corresponding to  $-\text{C}=\text{C}$ - stretching of the benzene ring,  $-\text{C}-\text{N}$  (the valence vibration of  $\text{C}-\text{N}$  bond of carbazole), and  $-\text{C}-\text{H}$  (out-of-plane deformation of  $\text{C}-\text{H}$  bond in the benzene ring). This provides further evidence of polymer formation. The most characteristic difference in the copolymer is the lack of bands at 690  $\text{cm}^{-1}$  ( $-\text{C}-\text{H}$  bending of trisubstituted aromatic rings) and 1378-1330  $\text{cm}^{-1}$  ( $-\text{C}-\text{N}$  stretching of aromatic  $\text{C}-\text{N}$  bonds or vibration of disubstituted benzene ring), which is characteristic of P[N-MCz]. The peak at 2967  $\text{cm}^{-1}$  belongs to  $-\text{CH}_3$  ( $\text{sp}^3$   $\text{CH}$  stretching)<sup>26</sup>. In the case of the copolymer, in addition to the peaks mentioned above, there are some shifts or new peak formations corresponding to the interaction of the monomers. Tian and Zerbi have used a parameter called the effective conjugation coordinate to calculate IR spectra for N-MPy. In particular, Zerbi's calculations predict that as the conjugation length is increased the intensity of the anti-symmetric ring-stretching mode at 1556  $\text{cm}^{-1}$  will decrease relative to the intensity of the symmetric mode at 1453-1450  $\text{cm}^{-1}$ . As a result, the ratio of the intensities of the 1556  $\text{cm}^{-1}$  and 1453-1450  $\text{cm}^{-1}$  band in an experimental IR spectrum can be used to obtain a relative measure of the conjugation length<sup>27</sup>. The conjugated double bonds of the methylpyrrole ring absorb around 1100  $\text{cm}^{-1}$  as split into 3 peaks (1175, 1116 and 1043  $\text{cm}^{-1}$ )<sup>28</sup>, which is observed as 2 peaks (1165 and 1066  $\text{cm}^{-1}$ ) in the copolymer. The sharp peak at around 1783  $\text{cm}^{-1}$  corresponding to  $\text{C}=\text{O}$  in propylene carbonate (solvent) incorporates in the copolymer, which looks like the combination of the peaks at 1761  $\text{cm}^{-1}$  in the P[N-MCz] and 1780  $\text{cm}^{-1}$  and in P[N-MPy] disappears in the case of the copolymer. The peaks at 2967  $\text{cm}^{-1}$  (N-MCz)<sup>29</sup> and at 2968  $\text{cm}^{-1}$  (N-MPy) belong to  $\text{CH}_3$  and  $\text{CH}_2$  in the homopolymers. These peaks disappear in the copolymer.

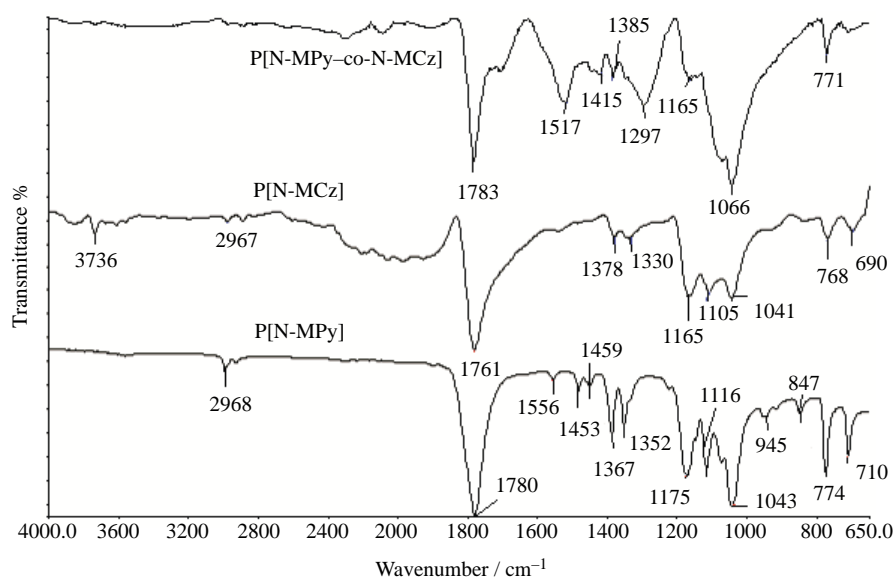


**Figure 11.** FTIR-ATR spectrum of P[N-MPy-co-N-MCz], P[N-MPy] and P[N-MCz] [N-MPy]<sub>0</sub> = 10<sup>-2</sup> M, [N-MCz]<sub>0</sub> = 10<sup>-2</sup> M in 0.1 M NaClO<sub>4</sub> / PC.

## UV-vis Spectrophotometric Results

### Ex-Situ Spectroelectrochemistry for coated polymer on ITO

P[N-MPy-co-N-MCz] films were deposited on ITO coated glass substrates potentiostatically at a constant potential (1.4 V) from a mixture of N-MPy and N-MCz monomers in 0.1 M NaClO<sub>4</sub>/ PC solution over 30 min (initial concentrations of monomers were 0.05 M). The ex-situ spectroelectrochemical spectrum of P[N-MPy-co-N-MCz] on ITO, by the formation of UV absorptions as the polymer becomes conducting and shows fast switching times (10 s) for the large optical changes being attained, is shown in Figure 12. The optical band gap of the film was 2.23 eV. In the fully reduced form at -1.2 V the polymer was yellow, but the color gradually changes to green by applying oxidizing potential (0.1 V) and at a higher potential it turns deep blue. This type of multicolor behavior is important for the preparation of electro-chromic materials.

The  $\pi - \pi^*$  transition of P[N-MPy] showed a maximum absorbance ( $\lambda_{max}$ ) at 446 nm (2.78 eV) (Figure 13a). The change in the band gap in the copolymer may stem from the incorporation of the N-MCz in the resulting polymer. It should also be noted that in the case of P[N-MPy-co-N-MCz] the polymer cannot be reduced completely as much as P[N-MPy], which also supports the incorporation of N-MPy in the polymer. Moreover, UV-vis peaks at lower energies in the oxidized state of both polymers make them useful for some applications in the near IR region. At this point, methylcarbazole brings an advantage, and the incorporation of it in the structure makes the polymer more flexible<sup>30</sup>. Electropolymerization of N-MCz was a little soluble in organic solvents (ACN and PC), which is coated on CFME. However, it is almost soluble in propylene carbonate, which is not coated on ITO.

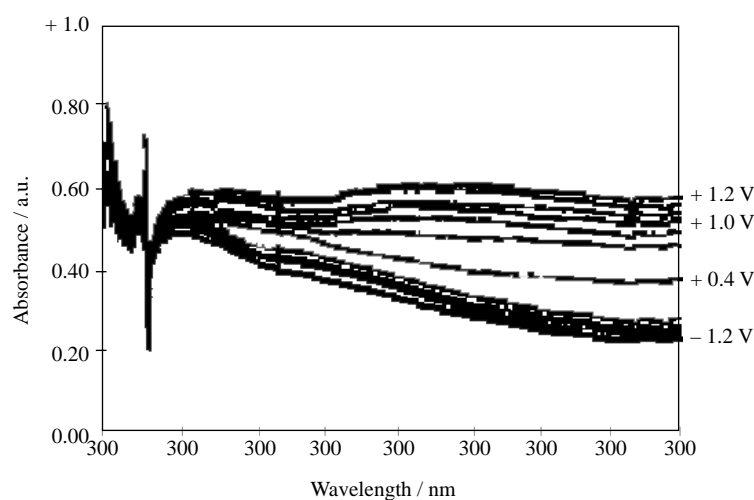


**Figure 12.** Ex-situ spectroelectrochemistry of P[N-MPy-co-N-MCz] film was obtained at different potentials in the range of -1.2 to +1.2 V on ITO [N-MCz]<sub>0</sub>/ [N-MPy]<sub>0</sub> = 1.

### Ex-Situ Spectroelectrochemistry for Soluble Species

The UV-visible spectrum of the copolymer with an increasing initial feed ratio of N-MCz indicated the use of ex-situ spectroelectrochemistry for soluble species (Figure 14). The UV-vis spectrum of solution is followed at one main peak ( $\lambda_1 = 678-688$  nm), which is probably due to co-oligomeric species. Therefore, as the methylcarbazole content increases in the initial feed ratio, absorbencies at  $\lambda_1 = 678-688$  nm increase (inset

of Figure 14). The maximum absorbance value of oligomers was also obtained for the copolymer at an initial feed ratio of  $[N-MCz]_0/[N-MPy]_0=1$  (Figure 14).

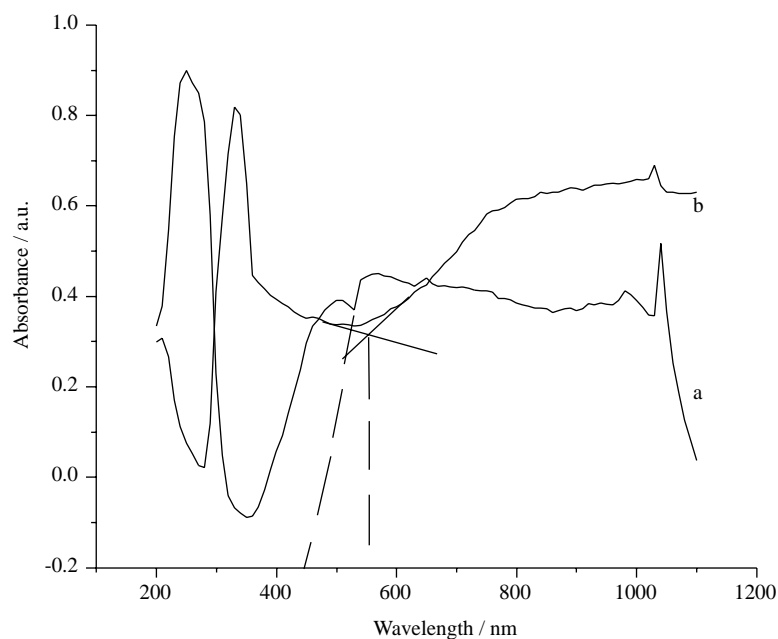


**Figure 13.** Ex-situ spectroelectrochemistry of a) neutral P[N-MPy] and b) neutral P[N-MPy-co-N-MCz] film obtained at different potentials in the range of -1.2 to +1.2 V.  $[N-MCz]_0/[N-MPy]_0 = 1$ ;  $[N-MPy]_0 = 5 \cdot 10^{-2}$  M.

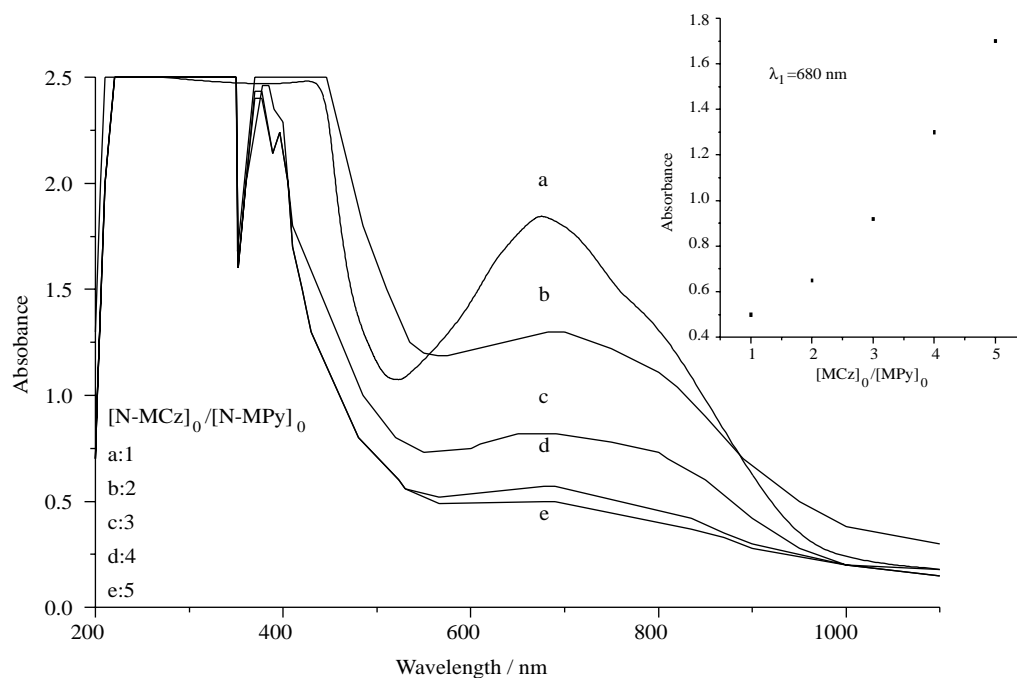


**Figure 14.** UV-vis spectrum of oligomeric species after polymerization with increasing amount of N-MCz. a)  $[N-MCz]_0/[N-MPy]_0 = 1$  b)  $[N-MCz]_0/[N-MPy]_0 = 2$  c)  $[N-MCz]_0/[N-MPy]_0 = 3$  d)  $[N-MCz]_0/[N-MPy]_0 = 4$  e)  $[N-MCz]_0/[N-MPy]_0 = 5$ .

## Stability of the Copolymer

The stability of the obtained copolymer, prepared in different electrolytes, was measured in a monomer-free electrolyte by the application of 50 cycles (Figure 15). When cycling proceeds, the current density decreases to a stable value. The polymer obtained in  $\text{LiClO}_4$  exhibited the most stable (minimum decreasing repetitive cycling) behavior. The copolymer in  $\text{LiClO}_4 / \text{ACN}$  has the highest stability according to the differences  $\Delta I_{p_a}$ , which is compared to  $\text{NaClO}_4$ , and  $\text{KClO}_4$  electrolytes in ACN.  $\Delta I_{p_a} (\text{LiClO}_4) = \sim 0.75 \mu\text{A cm}^{-2}$ ,  $\Delta I_{p_a} (\text{NaClO}_4) = \sim 2.2 \mu\text{A cm}^{-2}$ ,  $\Delta I_{p_a} (\text{KClO}_4) = \sim 1.25 \mu\text{A cm}^{-2}$  (Figure 16).

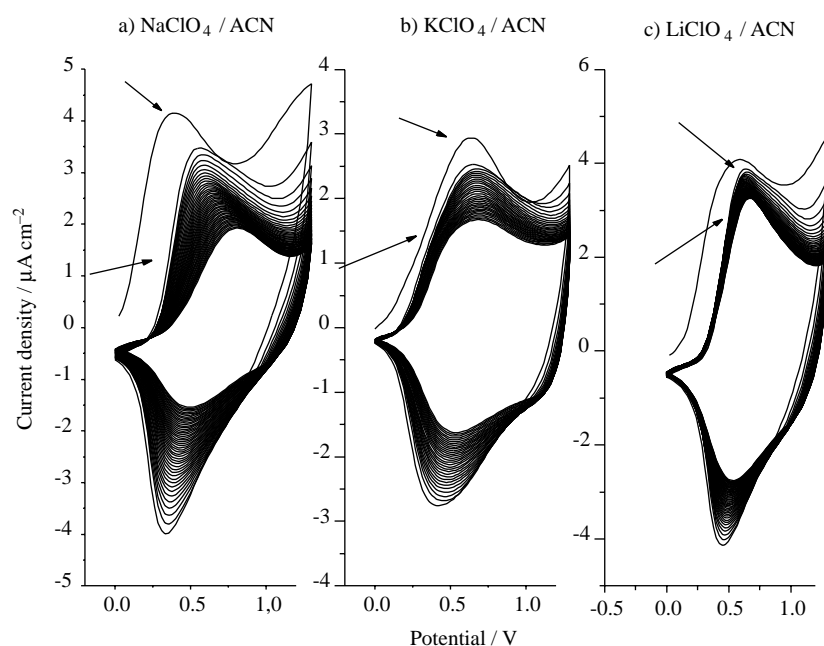


**Figure 15.** Stability test for P[N-MPy-co-N-MCz] potentiodynamically on CFME, using multiple cycles (50) in monomer free solution at  $100 \text{ mV s}^{-1}$ .  $[\text{N-MPy}]_0 = 10^{-3} \text{ M}$ ,  $[\text{N-MCz}]_0 = 10^{-3} \text{ M}$ . a)  $\text{NaClO}_4 / \text{ACN}$ , b)  $\text{KClO}_4 / \text{ACN}$ , c)  $\text{LiClO}_4 / \text{ACN}$ .

## Conclusion

In this study, the electrocopolymerization of N-MCz with N-MPy was studied to improve the properties of methylcarbazole. The oxidation potential of the copolymer film is lower than that of P[N-MCz] film. Electrochemical synthesis of the copolymer of methylpyrrole and methylcarbazole was achieved on CFMEs potentiodynamically. Upon repeated scans, new redox processes appeared at lower potentials, indicating the formation of an electroactive polymer film. The solid state conductivity measurements indicated that for the copolymer conductivity decreased with the increase in N-MCz concentration. The ex-situ UV-vis spectrum of the copolymer and 4-point probe conductivity measurements of the copolymer showed that when the initial feed ratio of  $[\text{N-MCz}]_0 / [\text{N-M-Py}]_0$  increases to 5, due to the disordered increase in the chain length of the polymer, conjugation decreases. This is shown in the conductivity ( $0.43 \text{ mS cm}^{-1}$ ) (Table 5).



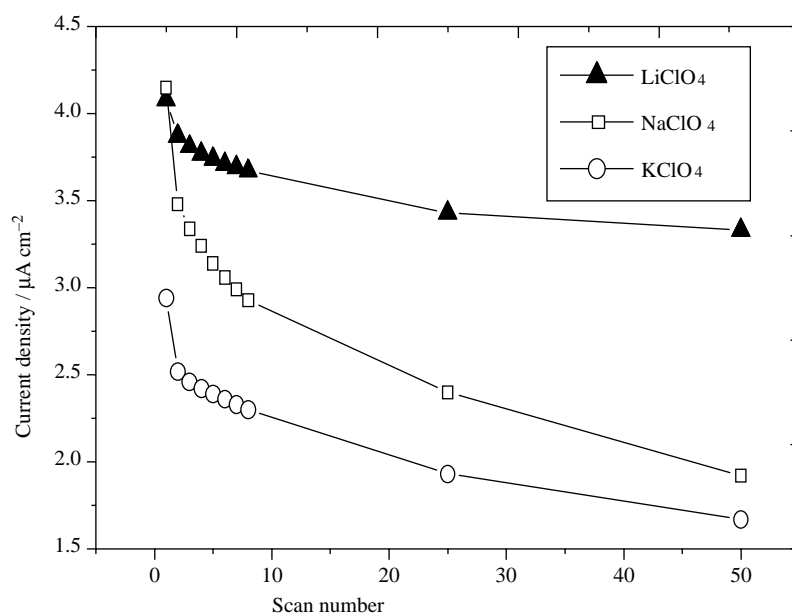


**Figure 16.** Anodic peak current densities of P[N-MPy-co-N-MCz] in different electrolytes using multiple cycles (50) in monomer-free solution at  $100 \text{ mV s}^{-1}$ ,  $[\text{N-MPy}]_0 = 10^{-3} \text{ M}$  and  $[\text{N-MCz}]_0 = 10^{-3} \text{ M}$ .

**Table 5.** UV-visible analysis of soluble copolymer or oligomers and 4-point probe conductivity measurement of P[N-MPy-co-N-MCz] while the amount of N-MCz increases.

$[\text{N-MCz}]_0 / [\text{N-MPy}]_0$	(Absorbance at 680 nm) <sup>a</sup>	Conductivity ( $\text{mS cm}^{-1}$ ) <sup>b</sup>
1	1.83	4.20
2	1.29	3.87
3	0.82	2.16
4	0.57	1.07
5	0.49	0.43

<sup>a</sup>Oligomeric soluble species

<sup>b</sup>Conductivities of copolymers are measured by obtaining free-standing film on stainless steel electrodes in 0.1 M  $\text{NaClO}_4 / \text{ACN}$ .

The choice of initial feed ratio, temperature and supporting electrolyte has an important influence on the electropolymerization behavior, with  $\text{LiClO}_4 / \text{ACN}$  being the most stable solvent of those tested (% loss of current density is minimum,  $\Delta I_{p_a} = \sim 0.75 \mu\text{A cm}^{-2}$ ).

## References

1. A.S. Sarac, “**Nanoscale spectroscopic characterization of conductive polymer electrocoated carbon fiber surface**”, in: HS. Nalwa (Ed.), *Polymeric Nanostructures*, 1st ed., (Chapter 16) American Scientific Publishers; Valencia, CA, USA, 2006.
2. A.S. Sarac, in: Herman, F. Mark (Ed.), “**Encyclopedia of Polymer Science and Technology**”, vol. 9, part 3, third ed., 2004.

3. H. Nishino, G. Yu, A.J. Heeger, T.A. Chen, R.D. Rieke, **Synth. Met.** **68**, 243-247 (1995).
4. H.Taoudi, J.C.Bernede, A.Bonnet, M.Morsli, and A.Goday, **Solid Thin Films**, **304**, 48-55 (1997).
5. M.C. Castej, C. Olivero, A. Fischer, S. Mausel, J. Michelson, D. Ades, A. Siove, **Appl. Surf. Sci.** **822**, 197-198 (2002).
6. S. Yapi.Abe, J.C. Bernede, M.A. Delvalle, Y. Tregouet, F. Ragot, F.R. Diaz, S. Lefrant, **Synth. Met.** **126**, 1-6 (2002).
7. A.S. Sarac, M. Ates and E.A. Parlak, **Int. J. Polym. Mater.** **53**, 785-798 (2004).
8. A.S. Sarac, M. Ates and E.A. Parlak, **Int. J. Polym. Mater.** **54**, 883-897 (2005).
9. A. Bismarck, A. Menner, J. Barner, A.F. Lee, K. Wilson, J. Springer, J.P. Rabe, and A.S. Sarac, **Surf. Coat. Technol.** **145**, 164-175 (2001).
10. E. Kumru, J. Springer, A.S. Sarac and A. Bismarck, **Synth. Met.** **123**, 391-402 (2001).
11. A.S. Sarac, A. Bismarck, E. Kumru and J. Springer, **Synth. Met.** **123**, 411-423 (2001).
12. A. Bismarck, A. Menner, E. Kumru, A.S. Sarac, M. Bistriz and E. Shulz, **J. Mater. Sci.** **37**, 461-471 (2002).
13. A.S. Sarac and J. Springer, **Surf. Coat. Technol.** **160**, 227-238 (2002).
14. E. Sezer, B. Ustamehmetoglu, A.S. Sarac, **Int. . Polym. Mater.** **53**, 105-118 (2004).
15. K. Faid, A. Siove, D. Ades, and C. Chevrot, and A. Siove, **Synth. Met.** **55**, 845-850 (1993).
16. M. Gerard, A. Chaubey and B.D. Malhotra, **Biosens. Bioelectron.** **17**, 345-359 (2002).
17. A.S. Sarac, U. Evans, M. Serantoni, J. Clohessy and V.J. Cunnane, **Surf. Coat. Technol.** **182**, 7-13 (2004).
18. A.S. Sarac, A. Bismarck, E. Kumru, J. Springer, **Synth. Met.** **123**, 411-423 (2001).
19. E. Kumru, J. Springer, A.S. Sarac, A. Bismarck, **Synth. Met.** **123**, 391-402 (2001).
20. A. Bismarck, A. Menner, J. Barner, A.F. Lee, K. Wilson and J. Springer, **Surf. Coat. Technol.** **145**, 164-175 (2001).
21. G. Sonmez, A.S. Sarac, **Synth. Met.** **135**, 459-460 (2003).
22. J.F. Rusling and S.L.Suib, **Adv. Mater.** **6**, 922-930 (1994).
23. A.S. Sarac, G. Sönmez and F.Ç. Cebeci, **J. App. Electrochem.** **33**, 295-301 (2003).
24. D. Obrien, A. Blayer, D. G. Lidzey, D. D. C. Bradly, T. Tsutsui, **J. Appl. Phys.** **82**, 2662-2672 (1997).
25. S. Janietz, D. D. C. Bradly, M. Grell, C. Giebeler, M. Inbasekaran, E.P. Woo, **Appl. Phys. Letters**, **73**, 2453-2454 (1998).
26. A.S. Sarac, M. Ates, and E.A. Parlak, **J. App. Electrochem.** **36**, 889-898 (2006).
27. J.T. Lei, Z. Cai and C.R. Martin, **Synth.Met.****46**, 53-59 (1992).
28. G. Sönmez, A.S. Sarac, **J. Mater. Sci.** **37**, 4609-4614 (2002).
29. E. Sezer, B. Ustamehmetoglu, A.S. Sarac, **Synth. Met.** **107**, 7-17 (1999).
30. A.S. Sarac, G. Sönmez and B. Ustamehmetoglu, **Synth. Met.** **98**, 177-182 (1999).